Creation of Artificial Surface Conductivity on Metallic Metamaterials

Masoud Edalatipour, Amin Khavasi, Mohsen Rezaei, and Khashayar Mehrany

***Abstract*—Metal films with a periodic arrangement of cut-through slits are studied to show that artificial surface conductivity is created at the flat interface between the periodic slits and the cover/substrate. The presence of surface conductivity when the periodic structure is modeled by an effective refractive index can describe how non-specular higher diffracted orders affect the specular zeroth diffracted order. The magnitude of this surface conductivity is controlled geometrically. The artificial surface conductivity is pure imaginary and thus reactive if all non-specular orders are evanescent. This is usually the case in the low frequency regime. At higher working frequencies when some non-specular diffracted orders are non-evanescent, however, the artificial surface conductivity becomes complex and thus resistive. The power lost in the resistive part of the surface conductivity represents the power, which is carried away from the specular direction.**

***Index Terms*—Metals, metamaterial, optical components, periodic structures, physical optics.**

I. Introduction

SUB-WAVELENGTH features in metallic films permit the synergistic combination of plasmonic and non-plasmonic properties, and thereby help us to achieve unusual traits that cannot be found in nature. Engineering of microstructures in metals has therefore been the subject of intensive research in the past few years [1]–[5]. Given that there is a demand for electromagnetic metamaterials at the terahertz frequency range, however, particular attention is more recently directed toward terahertz frequencies [6]–[11]. The creation of arbitrary high positive refractive index is a notable example that can bring forth a plethora of new possibilities, e.g., in further miniaturization of terahertz devices, enhancement of terahertz imaging resolution, and slow electromagnetic wave applications [12]–[14]. For instance, metallic films made of a periodic arrangement of holes/slits have already proved to be capable of creating an artificially high positive refractive index at terahertz frequencies—thanks to the existence of subwavelength propagating modes supported by highly conductive walls [15]–[17]. It is the aim of this manuscript to show that non-negligible surface conductivity is artificially induced on the metamaterial film of high index of refraction, whenever the working frequency is increased beyond a certain level. It will be shown that the magnitude of the effective surface conductivity being artificially induced on the film is proportional to the effective refractive index of the film and—much like the artificial high index of refraction—is geometrically controllable. Consideration of the artificial surface conductivity has two-fold significance. First, it improves the accuracy of modeling metallic metamaterials. Second, it is interesting and important in its own right because violating the continuity condition of the transverse magnetic field—which is caused by the artificially induced surface current—has numerous applications [18]–[21].

The paper is organized as follows: Section II is devoted to the detailed description of how the proposed artificial surface conductivity can account for the non-specular diffracted orders. Two different models: isotropic and anisotropic are provided. Numerical results are then given in Section III, where the efficiency of using artificial surface conductivity to take into account the effects of non-specular diffracted orders is demonstrated by comparing the obtained results against the numerical results found by using a rigorous approach. Finally, the conclusions are made in Section IV.

II. Artificial Surface Conductivity

For simplicity's sake, the most elementary, yet the most frequently cited case, is considered in this paper. It is a simple structure made of a periodic arrangement of vertical slits in a perfect metal film at free space [see Fig. 1(a)]. It can be effectively regarded as an isotropic nonmagnetic dielectric film of high refractive index when it is illuminated by normal incident wave and when it has small d/λ_0 and high aspect ratio d/a [15] (a is the periodicity of the structure and λ_0 is the free space wavelength of the incident wave). Although the effects of tilting the incident angle and decreasing the aspect ratio d/a are already modeled by introduction of magnetic anisotropy [15], [16], the effects of increasing the normalized frequency as embodied in the presence of more important higher order evanescent modes are not considered in the existing models based on the idea of using effective refractive index. Although higher reflected Floquet orders remain evanescent for $d/\lambda_0 < 1$, all the proposed models become erroneous when the working frequency is increased. This point is addressed in this section, where a nonzero surface conductivity is added to the interface of the already proposed models, i.e., the dielectric slab of nonmagnetic high refractive index film or the anisotropic magnetic film. In this fashion, the effects of higher Floquet orders are taken into account.

Assuming that a uniform P-polarized plane wave (the magnetic field along the y axis) is incident upon the perfect metal

Manuscript received January 01, 2012; revised February 14, 2012; accepted February 14, 2012. Date of publication February 28, 2012; date of current version April 06, 2012.

The authors are with the Electrical Engineering Department, Sharif University of Technology, Tehran 11155-4363, Iran (e-mail: edalatipour@ee.sharif.ir; a.khavasi@yahoo.com; mohsenr1986@gmail.com; mehrany@sharif.edu).

Color versions of one or more of the figures in this paper are available online at http://ieeexplore.ieee.org.

Digital Object Identifier 10.1109/JLT.2012.2188499

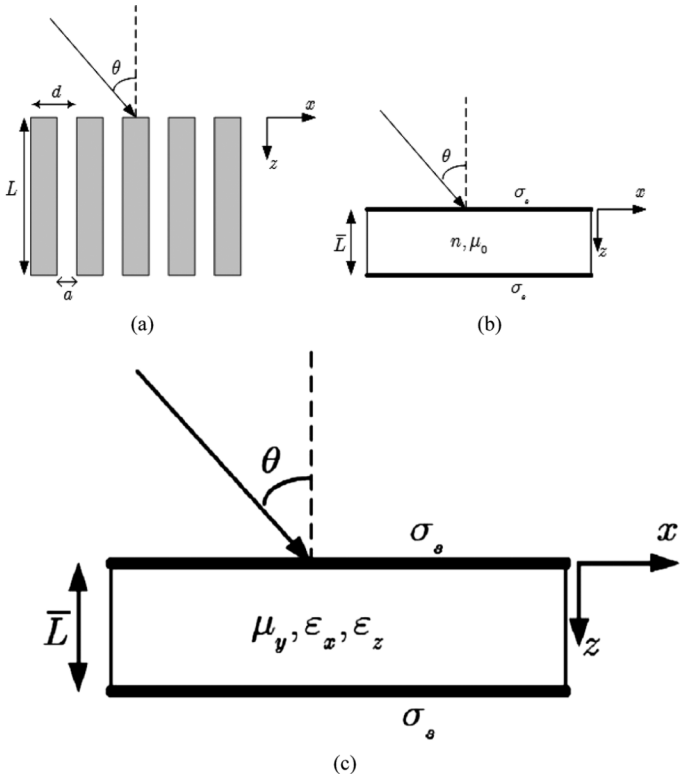

Fig. 1. (a) Periodic arrangement of cut-through slits in a metallic film, (b) the equivalent isotropic model with surface conductivity σ_s, and (c) the equivalent anisotropic model with surface conductivity σ_s.

film with cut-through slits shown in Fig. 1(a), the mth transmission diffraction order can be easily obtained when the TEM mode (electric field being along the x axis) is dominant in the empty space between the metallic slits [22]:

$$t_m = \frac{4s_0 \frac{k_0}{k_{zm}} s_m}{(1+\alpha)^2 e^{jk_0 L} - (1-\alpha)^2 e^{-jk_0 L}}. \tag{1}$$

Here, k_0 is the wave-number at free space

$$s_m = \sqrt{\frac{a}{d}} \frac{\sin(\frac{k_{xm}a}{2})}{\frac{k_{xm}a}{2}} \tag{2a}$$

$$\alpha = \sum_{p=-\infty}^{+\infty} \frac{k_0}{k_{zp}} s_p^2 \tag{2b}$$

$$k_{xm} = k_x + m\frac{2\pi}{d}, m = 0, \pm 1, \pm 2, \ldots \tag{2c}$$

$$k_{zm} = \sqrt{k_0^2 - k_{xm}^2} \tag{2d}$$

where k_x and k_z are the x and z component of the incident wave-vector, respectively.

The non-evanescent zeroth order transmission coefficient is then as follows:

$$t_0 = \frac{4\frac{k_0}{k_z} s_0^2}{\left(1 + \sum_p \frac{k_0}{k_{zp}} s_p^2\right)^2 e^{jk_0 L} - \left(1 - \sum_p \frac{k_0}{k_{zp}} s_p^2\right)^2 e^{-jk_0 L}}. \tag{3}$$

It is already shown that the transmission coefficient of a nonmagnetic dielectric film of appropriate high refractive index and that of an anisotropic magnetic film both match the zeroth transmission coefficient of the structure, when the working frequency is low enough to ignore the effects of higher diffracted orders. In the following subsections, an artificial surface conductivity is introduced to improve the accuracy of the already proposed models, when the working frequency is increased.

A. Isotropic Model

The structure in Fig. 1(a) is first modeled by a nonmagnetic dielectric film of high refractive index, on whose surface a nonzero surface conductivity exists. In accordance with Fig. 1(b), the proposed model consists of a dielectric film of thickness $\bar{L}$, refractive index n, permeability μ_0, and conducting interfaces that can support a surface current, J_s. The magnitude of the surface current is proportional to the surface conductivity, σ_s, and the tangential electric field along the x axis, E_x, i.e., $J_s = \sigma_s E_x$. The presence of surface conductivity alters the continuity condition of tangential magnetic field and enforces a discontinuity which is determined by the surface current J_s [19]–[21]. The transmission coefficient of this structure illuminated by the same uniform P-polarized plane wave then depends on σ_s and is as follows:

$$\bar{t}_0 = \frac{4\alpha}{(1+\alpha+\alpha\gamma)^2 e^{j\bar{k}_z \bar{L}} - (1-\alpha-\alpha\gamma)^2 e^{-j\bar{k}_z \bar{L}}} \tag{4}$$

where $\bar{k}_z = k_0\sqrt{n^2 - \sin^2(\theta)}$ is the z component of the wave vector in the high refractive index film, $\alpha = \bar{k}_z/(n^2 k_z)$ and $\gamma = \sigma_s k_z/(\omega\varepsilon_0)$ (ω and ε_0 are the angular frequency, and the permittivity of the free space, respectively). This equation can be straightforwardly obtained by solving the Maxwell's equations and applying the appropriate boundary conditions as presented in [19].

Comparison of the zeroth order transmission coefficient of the original structure in Fig. 1(a), i.e., (3), and that of the isotorpic model shown in Fig. 1(b), i.e., (4), confirms the equivalence of the isotropic model and the periodic film whenever we set

$$\begin{aligned} \alpha &= s_0^2 \frac{k_0}{k_z} \\ \bar{k}_z \bar{L} &= k_0 L \\ \alpha\gamma &= \sum_{p,p\neq 0} s_p^2 \frac{k_0}{k_{zp}}. \end{aligned} \tag{5}$$

Further simplification of the above-mentioned expressions for small angle of incidence shows that

$$\begin{aligned} n &= \frac{d}{a} \\ \bar{L} &= \frac{L}{n} \\ \sigma_s^p &= \frac{\omega\varepsilon_0}{s_0^2} \frac{s_p^2}{k_{zp}} \\ \sigma_s &= \sum_{p,p\neq 0} \sigma_s^p. \end{aligned} \tag{6}$$

It is noteworthy that the effective refractive index, n, and the thickness of the proposed model, $\bar{L}$, are not different from

what have been already reported [15]. Therefore, the presence of higher diffracted orders does not change the bulk parameters of the isotropic model. It can, however, drastically change the value of the surface conductivity. The contribution of the pth diffraction order in the overall surface conductivity is denoted by σ_s^p. For subwavelength slits, in particular, we have $k_x a \ll 1$ and σ_s^p is

$$\sigma_s^p = \frac{j}{\eta_0} \frac{\left(\sin \mathrm{c}\left(p\frac{a}{d}\right)\right)^2}{\sqrt{\left(\sin(\theta) + p\frac{\lambda_0}{d}\right)^2 - 1}} \tag{7}$$

where η_0 stands for the free intrinsic impedance. As expected, the contribution of the pth diffraction order in the overall surface conductivity is symmetric under normal incidence condition and thus we have $\sigma_s^{-p} = \sigma_s^p$. This expression stands witness for the fact that σ_s^p is purely reactive when the pth diffracted order is evanescent, i.e., when the normalized frequency is below the pth cut-off value:

$$\frac{d}{\lambda_0} < f_c^p = \frac{|p|}{1 - \mathrm{sgn}(p)\sin(\theta)}. \tag{8}$$

Purely reactive σ_s^p translates to a quadrature phase difference between the surface current supported by the pth diffracted order, and the tangential electric field. The losslessness is thus guaranteed for normalized frequencies lying below the first normalized cut-off frequency, i.e., when all non-specular orders are evanescent and $f < f_c^{-1} = 1/(1 + \sin(\theta))$. It should be however pointed out that when the normalized frequency gets close to the first normalized cut-off frequency from below, the magnitude of the reactive surface conductivity becomes non-negligible; thus, a modest error is incurred upon the already proposed model, wherein the reactive surface conductivity has been neglected. As the normalized frequency goes beyond the first normalized cut-off frequency, the artificial surface conductivity becomes resistive and thus the incurred error in neglecting surface conductivity is significantly increased. In point of fact, the already proposed model fails to consider the non-zero diffraction efficiency of non-specular orders but the proposed model considers the power lost to non-specular diffracted orders. This is due to the fact that the effective surface conductivity in the proposed model can become resistive. This point is shown through miscellaneous examples in Section III.

B. Anisotropic Model

Although the parameters of the proposed model in the previous subsection are extracted at normal incidence condition, its accuracy is preserved even for oblique incident angles because d/a is usually high enough to mimic high refractive index film [15]. It is however straightforward to follow the method of [16] and employ an anisotropic model with diagonal permittivity and permeability tensors to account for oblique incident angles even for not large enough values of d/a. A nonzero surface conductivity should however be considered at the upper and lower interfaces of the anisotropic model to take into account the effects of non-specular orders.

In accordance with Fig. 1(c), the thickness and the surface conductivity of the model are denoted by $\bar{L}$ and σ_s, respectively. The relevant elements of the permeability and permittivity tensors in the proposed model are μ_y, ε_x and ε_z because the magnetic field for the P-polarized waves is along the y-axis. The transmission coefficient of the model is as follows:

$$\bar{t}_0 = \frac{4\alpha}{(1+\alpha+\alpha\gamma)^2 e^{j\bar{k}_z\bar{L}} - (1-\alpha-\alpha\gamma)^2 e^{-j\bar{k}_z\bar{L}}} \tag{9}$$

where

$$\frac{\bar{k}_z^2}{\varepsilon_x \mu_y} + \frac{k_x^2}{\varepsilon_z \mu_y} = k_0 \tag{10}$$

and $\bar{k}_z$ is the z component of the wave vector in the anisotropic film, $\alpha = \bar{k}_z/\varepsilon_x k_z$ and $\gamma = \sigma_s k_z/\omega\varepsilon_0$. This time, the comparison between the zeroth order transmission coefficient of the original structure in Fig. 1(a), i.e., (3), and the transmission coefficient of the anisotropic model shown in Fig. 1(c), i.e., (9), confirms the equivalence of the anisotropic model and the original periodic structure. It can be easily shown that the sought-after parameters of the proposed model are as follows:

$$\begin{aligned} \varepsilon_x &= \frac{L}{\bar{L}}\frac{d}{a} \\ \varepsilon_z &= \infty \\ \mu_y &= \frac{L}{\bar{L}}\frac{a}{d} \\ \sigma_s^p &= \frac{\omega\varepsilon_0}{s_o^2}\frac{s_p^2}{k_{zp}} \\ \sigma_s &= \sum_{p, p\neq 0} \sigma_s^p. \end{aligned} \tag{11}$$

Interestingly, including the surface conductivity of the previous subsection in the already proposed anisotropic model given in [16] can accurately take into account the effects of oblique incident angles even when d/a is not very large.

III. Numerical Examples

In accordance with Fig. 1(a), we set $d = 200\ \mu$m, $a = 50\ \mu$m, $L = 300\ \mu$m and $\theta = 0$ for the first numerical example. The zeroth transmitted-order diffraction efficiency of the structure is calculated by using four different methods: the rigorous full-wave solution when perfect conductor is replaced by aluminum [23], [24], the single mode solution based on the TEM mode supported by perfect conductor slits, i.e., (3), the non-magnetic isotropic model proposed in [15], and the non-magnetic isotropic proposed model using σ_s^{+1} and σ_s^{-1} only. The obtained results are plotted versus normalized frequency and incident angle in Fig. 2(a) and (b), respectively. Fig. 2(a) shows that while the non-magnetic isotropic model in [15] is erroneous for $d/\lambda > 0.15$, the proposed model is fairly accurate even if there are only two terms retained in the surface conductivity expression given in (6). Fig. 2(b) shows that the superiority of the proposed model is preserved at different incident angles.

Increasing the normalized frequency beyond $d/\lambda = 1$ at normal incidence condition gives rise to non-evanescent non-specular orders; yet, the proposed model with σ_s^{+1} and σ_s^{-1}

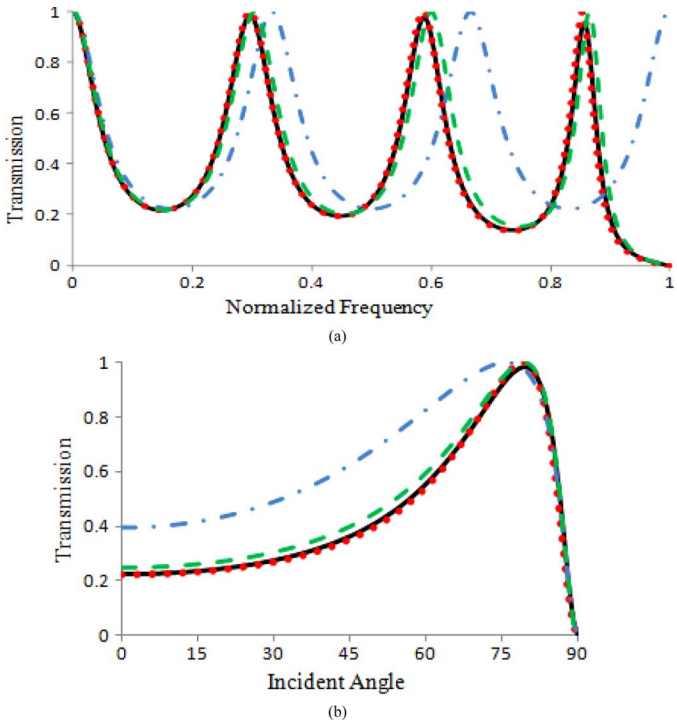

Fig. 2. Zeroth transmitted-order diffraction efficiency versus (a) normalized frequency (d/λ) at normal incidence, (b) incident angle at $d/\lambda = 0.41$: the full-wave solution (solid), the TEM single mode model (dotted), the conventional isotropic model (dashed-dotted), and the here proposed technique (dashed).

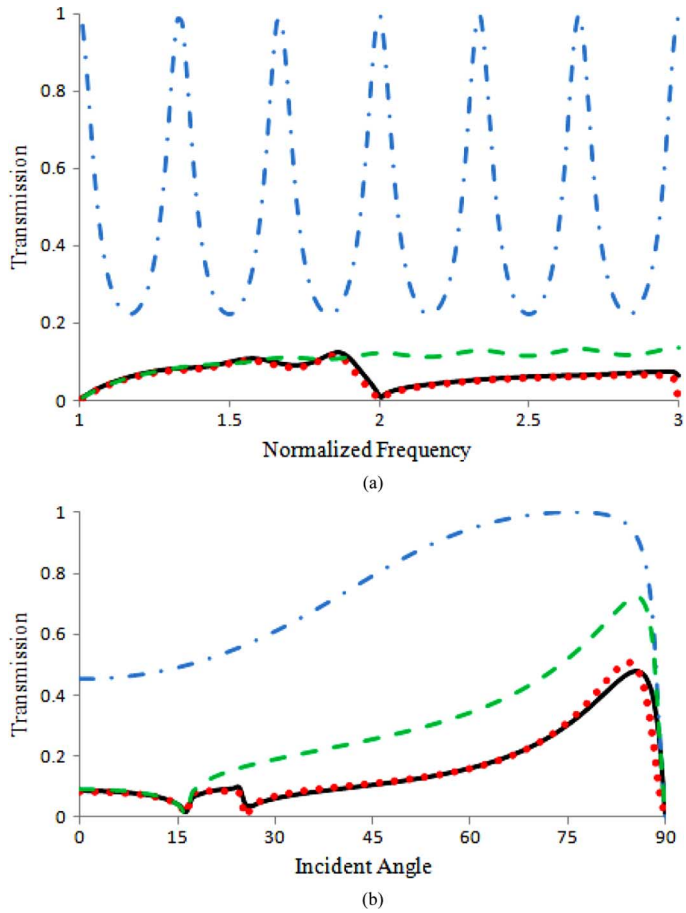

Fig. 3. Zeroth transmitted-order diffraction efficiency versus (a) normalized frequency (d/λ) at normal incidence, (b) incident angle at $d/\lambda = 1.4$ the full-wave solution (solid), the TEM single mode model (dotted), the conventional isotropic model (dash-dotted), and the here proposed technique (dashed).

continues to provide accurate results even for normalized frequencies as high as $\mathrm{d}/\lambda = 1.85$. This is numerically demonstrated in Fig. 3(a), where the zeroth transmitted-order diffraction efficiency of the structure is once again calculated by using the same methods. This figure shows while the original model is accurate when the normalized frequency is sufficiently below the first normalized cut-off frequency at $\mathrm{d}/\lambda = 1$, the proposed model with σ_s^{+1} and σ_s^{-1} remains accurate when the normalized frequency is sufficiently below the second normalized cut-off frequency at $\mathrm{d}/\lambda = 2$. It should be however noted that the first and second normalized cut-off frequencies are angle-dependent for oblique incident angles. The accuracy of the proposed model is subjected to the value of the incident angle. This is shown in Fig. 3(b), where normalized frequency is fixed at $\mathrm{d}/\lambda = 1.4$ and the zeroth transmitted-order diffraction efficiency of the structure is plotted versus incident angle. A considerable error is incurred when the incident angle gets close to 25.38° because the second normalized frequency is $\mathrm{d}/\lambda = 1.4$ at $\theta = 25.38°$. For incident angles beyond $\theta_{-2} = 25.38°$, the contribution of the not-included (-2)th diffracted order should be taken into account because σ_s^{-2} becomes resistive.

Since the error of the proposed model having only two terms σ_s^{+1} and σ_s^{-1} can be attributed to the considerable contribution of the second diffraction orders, inclusion of σ_s^{+2} and σ_s^{-2} is expected to rectify the obtained results. This is demonstrated in Fig. 4(a), where the zeroth transmitted-order diffraction efficiency of the structure is plotted by using the rigorous full-wave solution [23], [24], the non-magnetic isotropic model proposed in [15], and the proposed model with $\sigma_s^{+1}, \sigma_s^{-1}, \sigma_s^{+2}$ and σ_s^{-2} only. A close examination of the obtained results shows that 1) the incurred error at normal incidence is less than 4.8% for normalized frequencies up to $d/\lambda = 2.94$, and 2) the incident angle at the fixed normalized frequency of $d/\lambda = 1.4$ can go beyond $\theta_{-2} = 25.38°$.

These examples show that even though the parameters of the proposed model are extracted at normal incidence condition, the accuracy of the model is preserved for oblique incident angles. This is due to the fact that d/a is usually high enough to mimic high refractive index films [15]. As the final example, the zeroth order transmission coefficients are compared for small d/a, when the already proposed models should be anisotropic. The zeroth transmitted diffracted-order is plotted versus incident angle in Fig. 5. The results are obtained by using the already proposed anisotropic model given in [18], the proposed isotropic model including $\sigma_s^{+1}, \sigma_s^{-1}, \sigma_s^{+2}$ and σ_s^{-2}, the proposed anisotropic model including $\sigma_s^{+1}, \sigma_s^{-1}, \sigma_s^{+2}$ and σ_s^{-2}, and the full-wave solution [23], [24]. This figure shows that, first, the contribution of surface conductivity outweighs the contribution of anisotropy, and second, the performance of the anisotropic model with surface conductivity is no better than that of the already proposed anisotropic model if the angle of incidence is close to the grazing angle.

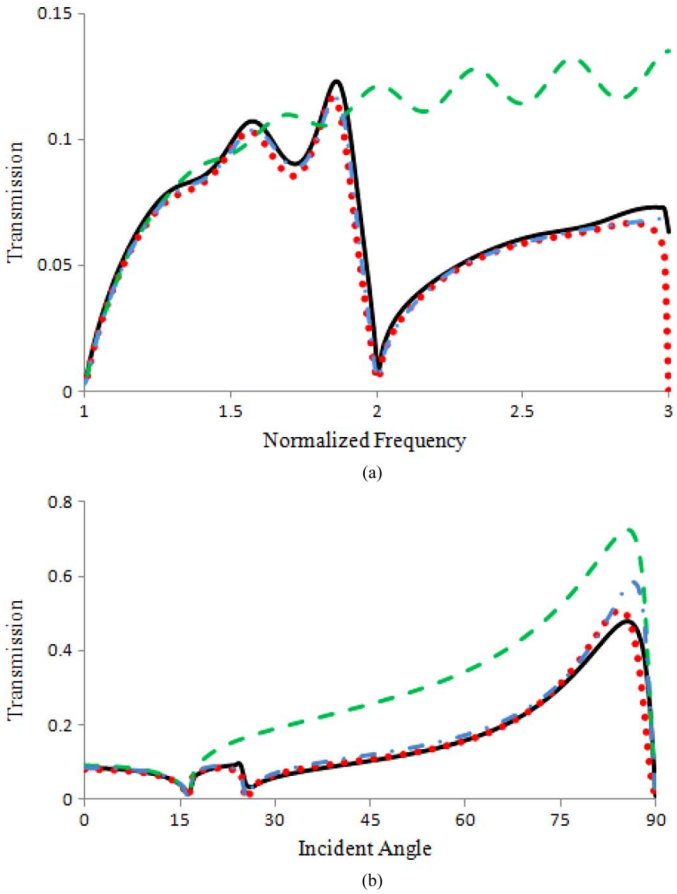

Fig. 4. Zeroth transmitted-order diffraction efficiency versus (a) normalized frequency (d/λ) at normal incidence, (b) incident angle at $d/\lambda = 1.4$: the full-wave solution (solid), the TEM single mode model (dotted), the here proposed technique with σ_s^{+1} and σ_s^{-1} only (dashed), and the here proposed technique with σ_s^{+1}, σ_s^{-1} and σ_s^{+2}, σ_s^{-2} only (dashed-dotted).

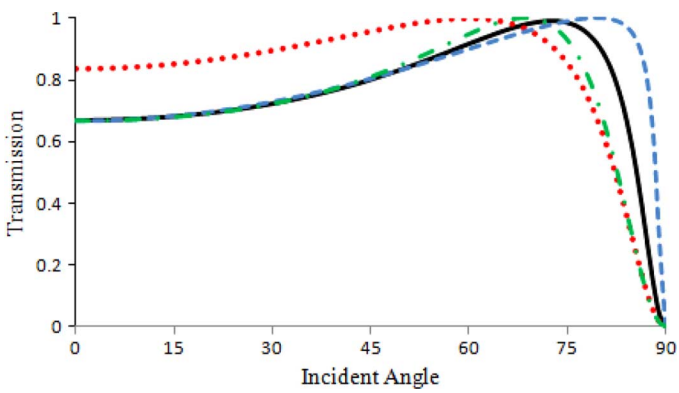

Fig. 5. Zeroth transmitted-order diffraction efficiency versus incident angle at $d/\lambda = 1.4$ and $d/a = 2$: the full-wave solution (solid), the conventional anisotropic model [16] (dotted), the here-proposed isotropic model (dashed), and the anisotropic model with surface conductivity (dashed-dotted).

IV. Conclusion

In conclusion, we considerably improved the effective medium approximation of metallic metamaterials for the frequencies up to the THz regime, where the metallic region can still be reasonably approximated by perfect conductor. It is worth noting that the proposed model is applicable whenever the ohmic loss or plasmonic effects of metals are negligible, i.e., at microwave and near infrared frequencies. It is also worth noting that further improvement is still possible by employing the proposed methodology to redress the effective surface conductivity by including the effects of non-TEM modes, which exist between the metallic slits in the structure.

It should be finally pointed out that the importance of the proposed model for the elementary structure shown in Fig. 1(a) lies in illustrating that the presence of surface conductivity can considerably improve the accuracy of the homogenization schemes. Thanks to the significant contribution of surface conductivity in modeling higher normalized frequencies, more complex structures, e.g., perforated metals with two-dimensional periodicity, can also be more accurately homogenized.

References

[1] P. Belov and Y. Hao, "Subwavelength imaging at optical frequencies using a transmission device formed by a periodic layered metal-dielectric structure operating in the canalization regime," *Phys. Rev. B*, vol. 73, no. 11, pp. 113110–113113, 2006.

[2] C. Min, P. Wang, C. Chen, Y. Deng, Y. Lu, H. Ming, T. Ning, Y. Zhou, and G. Yang, "All-optical switching in subwavelength metallic grating structure containing nonlinear optical materials," *Opt. Lett.*, vol. 33, no. 8, pp. 869–871, 2008.

[3] H. Kim, J. Park, and B. Lee, "Tunable directional beaming from subwavelength metal slits with metal—Dielectric composite surface gratings," *Opt. Lett.*, vol. 34, no. 17, pp. 2569–2571, 2009.

[4] J. Shin, J.-T. Shen, and S. Fan, "Three-dimensional electromagnetic metamaterials that homogenize to uniform non-Maxwellian media," *Phys. Rev. B*, vol. 76, no. 11, pp. 113101–113104, 2007.

[5] C. Cheng, J. Chen, D. J. Shi, Q. Y. Wu, F. F. Ren, J. Xu, Y. X. Fan, J. Ding, and H. T. Wang, "Physical mechanism of extraordinary electromagnetic transmission in dual-metallic grating structures," *Phys. Rev. B*, vol. 78, no. 7, pp. 075406–075414, 2008.

[6] Y. Todorov, L. Tosetto, J. Teissier, A. M. Andrews, P. Klang, R. Colombelli, I. Sagnes, G. Strasser, and C. Sirtori, "Optical properties of metal-dielectric-metal microcavities in the THz frequency range," *Opt. Express*, vol. 18, no. 13, pp. 13886–13907, 2010.

[7] C. W. Berry, J. Moore, and M. Jarrahi, "Design of reconfigurable metallic slits for terahertz beam modulation.," *Opt. Express*, vol. 19, no. 2, pp. 1236–1245, 2011.

[8] J. Pendry, L. Martin-Moreno, and F. Garcia-Vidal, "Mimicking surface plasmons with structured surfaces," *Science*, vol. 305, no. 5685, p. 847, 2004.

[9] F. J. Garcia-Vidal, L. Martín-Moreno, and J. B. Pendry, "Surfaces with holes in them: New plasmonic metamaterials," *J. Opt. A: Pure Appl. Opt.*, vol. 7, no. 2, pp. S97–S101, Feb. 2005.

[10] D. Wu, N. Fang, C. Sun, and X. Zhang, "Terahertz plasmonic high pass filter," *App. Phys. Lett.*, vol. 83, no. 1, p. 201, 2003.

[11] X. Lu, J. Han, and W. Zhang, "Resonant terahertz reflection of periodic arrays of subwavelength metallic rectangles," *App. Phys. Lett.*, vol. 92, no. 12, p. 121103, 2008.

[12] J. Shin, J.-T. Shen, and S. Fan, "Three-dimensional metamaterials with an ultrahigh effective refractive index over a broad bandwidth," *Phys. Rev. Lett.*, vol. 102, no. 9, p. 093903, Mar. 2009.

[13] P. B. Catrysse, J. Shen, G. Veronis, H. Shin, and S. Fan, "Metallic metamaterials with a high index of refraction," *Opt. Photon. News*, vol. 17, no. 12, pp. 34–34, 2006.

[14] M. Choi, S. H. Lee, Y. Kim, S. B. Kang, J. Shin, M. H. Kwak, K. Y. Kang, Y. H. Lee, N. Park, and B. Min, "A terahertz metamaterial with unnaturally high refractive index," *Nature*, vol. 470, no. 7334, pp. 369–373, 2011.

[15] J. Shen, P. Catrysse, and S. Fan, "Mechanism for designing metallic metamaterials with a high index of refraction," *Phys. Rev. Lett.*, vol. 94, no. 19, pp. 1–4, May 2005.

[16] J. Shin, J. T. Shen, P. B. Catrysse, S. Fan, and S. Member, "Cut-through metal slit array as an anisotropic metamaterial film," *Quantum*, vol. 12, no. 6, pp. 1116–1122, 2006.

[17] A. Pimenov and A. Loidl, "Experimental demonstration of artificial dielectrics with a high index of refraction," *Phys. Rev. B*, vol. 74, no. 19, pp. 193102–193104, 2006.

[18] Y. O. Averkov and V. M. Yakovenko, "Surface electromagnetic waves at an anisotropically conducting artificial interface," *Phys. Rev. B*, vol. 81, no. 4, pp. 045427–045433, 2010.

[19] K. Mehrany, S. Khorasani, and B. Rashidian, "Novel optical devices based on surface wave excitation at conducting interfaces," *Semicond. Sci. Technol.*, vol. 18, pp. 582–588, 2003.
[20] K. Mehrany and B. Rashidian, "Novel optical slow wave structure and surface electromagnetic wave coupler with conducting interfaces," *Semicond. Sci. Technol.*, vol. 19, pp. 890–896, 2004.
[21] K. Mehrany, S. Khorasani, and B. Rashidian, "Novel optical slow wave structure and surface electromagnetic wave coupler with conducting interfaces," in *Proc. SPIE*, 2003, vol. 4833, p. 776.
[22] P. Lalanne, J. P. Hugonin, S. Astilean, M. Palamaru, and K. D. Möller, "One-mode model and airy-like formulae for one-dimensional metallic gratings," *J. Opt. A: Pure Appl. Opt.*, vol. 2, no. 1, pp. 48–51, 2000.
[23] A. Khavasi and K. Mehrany, "Adaptive spatial resolution in fast, efficient, and stable analysis of metallic lamellar gratings at microwave frequencies," *IEEE Trans. Antennas Propag.*, vol. 57, no. 4, pp. 1115–1121, Apr. 2009.
[24] A. Khavasi and K. Mehrany, "Regularization of jump points in applying the adaptive spatial resolution technique," *Opt. Commun.*, vol. 284, p. 3211, 2011.

Masoud Edalatipour was born in Ghaenat, Iran, on March 6, 1985. He received the B.Sc. degree from Ferdowsi University of Mashhad, Mashhad, Iran, in 2007, and the M.Sc. degree from Sharif University of Technology, Tehran, Iran, in 2009, both in electrical engineering. He is currently working toward the Ph.D. degree at the Sharif University of Technology.

His research interest include terahertz, plasmonics, and photonics.

Amin Khavasi was born in Zanjan, Iran, on January 22, 1984. He received the B.Sc. and M.Sc. degrees from Sharif University of Technology, Tehran, Iran, in 2006 and 2008, respectively, both in electrical engineering. He is currently working toward the Ph.D. degree at the Sharif University of Technology.

His research interest include photonics, circuit modeling of photonic structures, and computational electromagnetic.

Mohsen Rezaei was born in Razan, Hamedan, Iran, on April 25, 1986. He received the B.Sc. degree from the Department of Electrical and Computer Engineering, University of Tehran, Tehran, Iran, in 2009. He is currently working toward the M.Sc. degree at the Sharif University of Technology, Tehran, Iran.

Since spring 2010, he has been a Research Assistant at the Integrated Photonic Laboratory at the Sharif University of Technology. His M.Sc. project is on the proposing transmission line models for the plasmonic structures.

Khashayar Mehrany was born in Tehran, Iran, on September 16, 1977. He received the B.Sc., M.Sc., and Ph.D. (*magna cum laude*) degrees from Sharif University of Technology, Tehran, Iran, in 1999, 2001, and 2005, respectively, all in electrical engineering.

Since then, he has been with the Department of Electrical Engineering, Sharif University of Technology, where he is at the moment an Associate Professor. His current research interests include photonics, plasmonics, and integral imaging.